



Porous-shaped n -CdZnO/ p -Si heterojunctions for UV photodetectors

Vijay S. Rana¹ · Jeevitesh K. Rajput^{1,2} · Trilok K. Pathak^{1,3} · L. P. Purohit¹

Received: 5 January 2021 / Accepted: 16 February 2021 / Published online: 3 March 2021
© The Author(s), under exclusive licence to Springer-Verlag GmbH, DE part of Springer Nature 2021

Abstract

In this study, n -type $\text{Cd}_y\text{Zn}_{1-y}\text{O}$ ($y=0, 0.5, 1, 1.5$ at%) thin films were deposited on p -Si and soda lime glass substrates using sol-gel spin coating technique. From the X-ray diffraction patterns, it was observed that all thin films had wurtzite structure with (002) orientation. Scanning electron micrograph results revealed that the morphology varied with higher Cd doping in ZnO. The bandgap was decreased from 3.29 eV (undoped ZnO) to 3.26 eV ($y=1.5$ at%) as Cd content increased. The electronic parameters of the $\text{Cd}_y\text{Zn}_{1-y}\text{O}$ ($y=1$ at%) thin film heterojunction such as ideality factor (η) and barrier height (Φ_B) were obtained using the thermionic emission theory as 2.53 and 0.70 eV, respectively. $\text{Cd}_y\text{Zn}_{1-y}\text{O}$ ($y=1$ at%) showed responsivity 0.01 A/W on 3.2 mW/cm² exposure of UV light (365 nm) at 4 V bias voltage. The heterojunction so formed seems to be an excellent candidate to be used as an optical sensor (UV photodetector) in optoelectronics.

Keywords CdZnO · Sol-gel · Heterojunction · I–V characteristics · Photodetection

1 Introduction

Ultraviolet (UV) photodetectors have wide features that are suitable to a variety of industrial applications including flame detection, water purification, money counting, ozone layer detection, missile warning systems and effects in modern life in healthcare setting [1, 2]. UV light can be used in the field of medical science including eczema facilitating eradicating germs, synthesizing vitamin and treatment of various diseases such as jaundice, cataracts and skin cancer [3, 4]. However, many hazards have occurred due to UV radiation such as jaundice, porphyria, lupus erythematosus and skin cancer [5, 6]. Heterojunction-based UV photodetectors show high rapid response and low dark current as compared to photoconductive detectors. Photoconductive detector is based on Photoconductive effect. In this detector, two ohmic contacts are made on the top of semiconductor material piece. Heterojunction detector is made of p – n

junction diode. Various semiconductors metal oxide-based UV photodetectors such titanium dioxide, gallium nitride and tin oxide [7–9] have been reported in the literature, but the low responsivity and poor compatibility are still a problem for their practical applications. Many research groups are trying to explore the ZnO (high exciton binding energy 60 meV at room temperature RT)-based UV photodetectors because it has low cost, high chemical, thermal and photoelectric stability [10, 11].

ZnO belongs to the II–VI group semiconductor with wide bandgap ($E_g=3.37$ eV) and it has many optoelectronic applications viz UV photodetectors, UV light-emitting diodes (LEDs), transparent conducting oxides and photodiode [12–17]. The bandgap of ZnO can be easily tuned by alloying Be, Mg, Ca and Cd elements [18, 19]. The bandgap of CdO (2.3 eV) is smaller as compared to ZnO (3.32 eV), so by Cd doping the bandgap of ZnO can be shifted from blue to red spectral range [20, 21] as the work function of CdO (3.4 eV) is less than ZnO (4.71 eV) [22, 23]. Usually, CdO shows intrinsically n -type semiconductor behaviour due to the native defects (oxygen vacancies and interstitials cadmium) [24]. In addition, the crystalline structure and lattice parameter of CdO are close to ZnO. Moreover, the doping of Cd with ZnO (controlling the native defects on doping of Cd with ZnO) is very useful for the fabrication of heterojunction and superlattice structures [25, 26].

✉ L. P. Purohit
proflppurohitphys@gmail.com; lppurohit@gkv.ac.in

¹ Semiconductor Research Lab, Department of Physics, Gurukula Kangri University, Haridwar, India

² Department of Physics, Babasaheb Bhimrao Ambedkar University, Lucknow, India

³ Department of Physics, TKCOE Teerthanker Mahaveer University, Moradabad, India

Several investigations were carried out on ZnO-based heterojunctions for photodetection of UV and visible light. The heterojunction of n -ZnO/ p -Si has many advantages, because of excellent quality (high exciton binding energy of ZnO and cheapness of Si substrate), cost-effectiveness, large wafer size, and most important the possibility of integrating oxide semiconductors which can be used in optoelectronic devices [20, 27]. Many researchers had worked on different types of heterojunctions viz. Kumar et al. [28] have worked n -type aluminium–boron-co-doped ZnO on p -type silicon (n -AZB/ p -Si) heterojunction diode and reported the ideality factor and potential barrier (at the junction) values 1.63 and 0.40 eV, respectively. Al-Hardan et al. [29] have worked on Ag/ZnO/ p -Si/Ag heterojunction with the ideality factor and potential barrier (at the ZnO/Si junction) 2.32 and 0.78 eV, respectively. Tataroglu et al. [22] have investigated photoconducting properties of $\text{Cd}_{0.4}\text{Zn}_{0.6}\text{O}/p$ -Si photodiode in which the ideality factor and potential barrier values were reported 5.80 and 0.80 eV, respectively. It is expected that the Cd concentration in ZnO could be a better option for making heterojunction diodes, n -ZnO/ p -Si [30–32].

There are very few reports published on Cd-doped ZnO thin films for photodetection applications using sol–gel technique. The sol–gel spin coating technique is easy for compositional modification, many variables to control film growth, composition fidelity, simple and inexpensive equipment, entropy of mixing, excellent control on stoichiometry and the ability to produce thin uniform films on large area substrates [25, 33, 34]. In this study, $\text{Cd}_y\text{Zn}_{1-y}\text{O}$ ($y=0, 0.5, 1, 1.5$ at%) thin films were deposited on p -Si and glass substrate by spin coating to analyse optical bandgap and morphological properties. Then, the electrical and photo-electrical properties of n -CdZnO/ p -Si heterojunction were examined using I–V measurement, in dark and illumination conditions under ambient light and UV light (365 nm).

2 Materials and methods

The $\text{Cd}_y\text{Zn}_{1-y}\text{O}$ thin films were deposited on p -Si (Inteligent Material Pvt. Ltd., Thickness ~ 200 – 500 μm and resistivity ~ 1 – 10 $\text{m}\Omega$ cm) and glass substrates prepared by the sol–gel method. Firstly, the precursor solution of ZnO 0.5 mol/l concentration was prepared by dissolving zinc acetate di-hydrate [$\text{Zn}(\text{CH}_3\text{COO})_2 \cdot 2\text{H}_2\text{O}$] in 2-methoxy ethanol and MEA was then added to this solution as a stabilizer. To deposit $\text{Cd}_y\text{Zn}_{1-y}\text{O}$ ($y=0, 0.5, 1, 1.5$ at% thin films coded as CZ-1, CZ-2, CZ-3 and CZ-4, respectively), the appropriate amount of cadmium acetate-dihydrate was mixed in this solution. After that, the solution was stirred using a magnetic stirrer to get the transparent solution. The Si substrates were first cut into 1×1 cm^2 pieces and cleaned by dipping in methanol, acetone and deionized water solution for 5 min in

an ultrasonic cleaner. The glass substrates were also cleaned by the same process. The prepared solution (approx. 0.5 ml) was dropped on the substrate and rotated at 2500 rpm for 30 s using a spin coater. After the deposition, the films were dried at 250 $^\circ\text{C}$ for 10 min into furnace. This procedure was repeated ten times. After that, the thin films were annealed in air at 450 $^\circ\text{C}$ for 1 h. The contacts were prepared by evaporating Al metal on the back of Si wafers and top contacts (Al metal) were prepared on $\text{Cd}_y\text{Zn}_{1-y}\text{O}$ thin films by the sputtering technique through a shadow mask.

The structural properties were studied using X-ray diffraction (XRD). The surface morphology of the films was investigated using a scanning electron microscopy (SEM). The optical transmittance spectra were collected using UV–Vis–IR spectrophotometer (Shimadzu, Japan). An ultra-violet LED with a wavelength of 365 nm and an intensity of 3.2 mW cm^{-2} was used as a UV light source. Electrical measurements were taken using electrometer (Keithley 4200 Semiconductor Characterization System). The experimental set-up for I–V measurements in dark and UV light is shown in Fig. 1.

3 Results and discussion

3.1 Structural properties

The phase and crystallinity of undoped and cadmium-doped ZnO thin films were analysed by XRD pattern. The structural studies of pure and Cd-doped ZnO thin films (CZ-1, CZ-2, CZ-3, CZ-4) are shown in Fig. 2. The XRD diffraction peaks of all thin films were obtained along (100), (002), (101) and some less intense peaks were observed at (110) and (102). XRD pattern shows a strong dominated orientation at (002) plane of all thin films samples. This study reveals that all thin films sample having hexagonal wurtzite

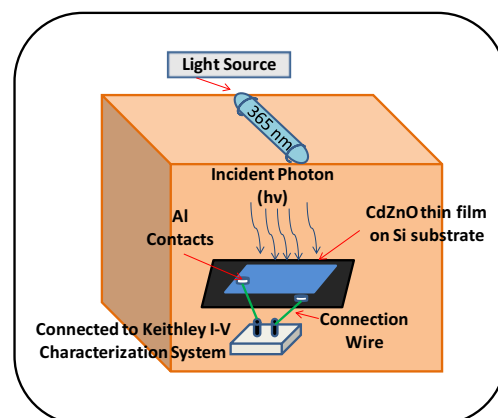


Fig. 1 The experimental set-up for the I–V measurements in dark and UV light (365 nm)

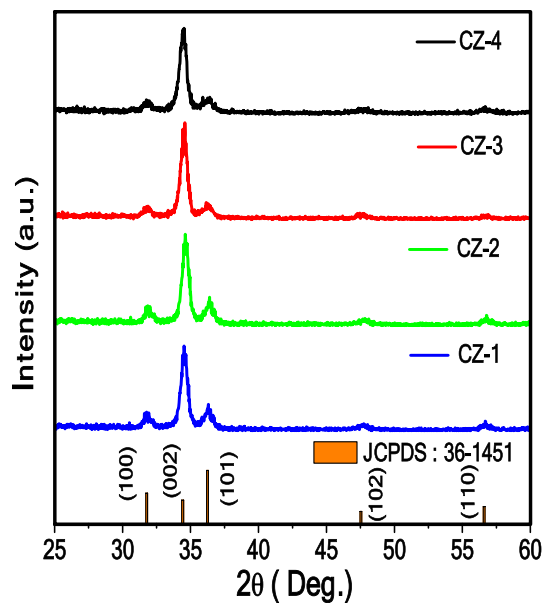


Fig. 2 X-ray diffraction patterns of $Cd_yZn_{1-y}O$ ($y=0$ (CZ-1), $y=0.5$ (CZ-2), $y=1$ (CZ-3), $y=1.5$ (CZ-4) at%) thin films on *p*-Si substrate with JCPDS 36-1451 in range of 25–60°

structure [19]. The lattice parameters ‘*c*’ and ‘*a*’ shown in Table 1 were calculated corresponding to (002) and (100) peaks [23]. The crystallite size of these films was calculated by using Debye–Scherrer’s formula [19] and is given in Table 1.

3.2 Surface morphology

The surface morphology of undoped and Cd-doped ZnO (CZ-1, CZ-2, CZ-3, CZ-4) thin films is shown in Fig. 3a–h. At high magnification, all films have wrinkle-type network micrographs. The wrinkle formation has been attributed to either the lack of hydroxide in the initial sol precursor or sintering temperature of thin films [35, 36]. From these figures, at high magnification all films have round- and oval-shaped nanocrystallite grains. In addition, all the films offer porous network, which is useful to enhance photodetection properties and passes more sites to react photon and adhered well to the substrate without any cracks [19, 24, 37].

Table 1 The structural and optical parameters of $Cd_yZn_{1-y}O$ thin films

Sample code	Peak position (2θ) (deg.)	FWHM (β) (deg.)	Lattice parameter (a) (Å)	Lattice parameter (c) (Å)	Crystallite size (nm)	Bandgap (E_g) (eV)
CZ-1	34.48	0.522	3.245	5.198	15.9	3.29
CZ-2	34.54	0.505	3.244	5.189	16.4	3.27
CZ-3	34.52	0.511	3.244	5.192	16.2	3.27
CZ-4	34.45	0.518	3.244	5.202	16.0	3.26

3.3 Optical properties

The optical properties were studied for undoped and Cd-doped ZnO (CZ-1, CZ-2, CZ-3, CZ-4) thin films deposited on glass substrates in place of Si substrate [22, 26]. The transmittance spectra of all films show that average transparency of the films was 85% in the visible region and very low in the ultraviolet region, and a sharp absorption edges in the ultraviolet region. The change in the absorption edge shows shift in the optical bandgap of samples. The decrease in average optical transmittance may be due to the thickness of the thin film and the Cd incorporation. [25, 34]. Singh et al. [23] in their work have also reported that the transmittance spectra of all thin films exhibit the average transparency 75% in the visible region. For the allowed direct transitions, optical bandgap of thin films was calculated from transmission spectra using Tauc’s plot method as shown in Fig. 4b [33]. It can be noticed that the bandgap decreases from 3.29 eV (undoped ZnO) to 3.26 eV ($y=1.5$ at%) as Cd content increased as shown in Table 1. The decreased bandgap of Cd-doped ZnO was expected due to CdO having smaller bandgap than ZnO [26].

3.4 Electrical properties and UV sensing measurement

Figure 5a, b shows the *I*–*V* characteristics of *n*- $Cd_yZn_{1-y}O$ /*p*-Si heterojunction diodes in dark and UV light (365 nm) with optical power density 3.2 mW/cm². The diodes show heterojunctions nature which was confirmed by the nonlinear *I*–*V* characteristic. The schematic diagram of diode structure is also shown in inset of Fig. 5c. The maximum forward current (I_f) was observed in the CZ-3 heterojunction. The rectification ratio (the ratio of the forward I_f to current and reverse current I_r) of the CZ-3 heterojunction at ± 4 V was approximately 2.22 and 26.63 in dark and UV light (365 nm), respectively. The turn-on voltages of the CZ-3 heterojunction were determined by extrapolating the *I*–*V* curve to the intersection of the abscissa 0.940 V and 1.21 V for dark and UV light, respectively, as shown in Fig. 5c [21]. Bougrine et al. [38] reported that the electrical resistivity of the films initially decreases with the addition of dopant ion, reaches a minimum value and then increases

Fig. 3 FE-SEM images of $\text{Cd}_y\text{Zn}_{1-y}\text{O}$ (CZ-1, CZ-2, CZ-3, CZ-4) thin films on *p*-Si substrate with 10KX and 50KX magnification

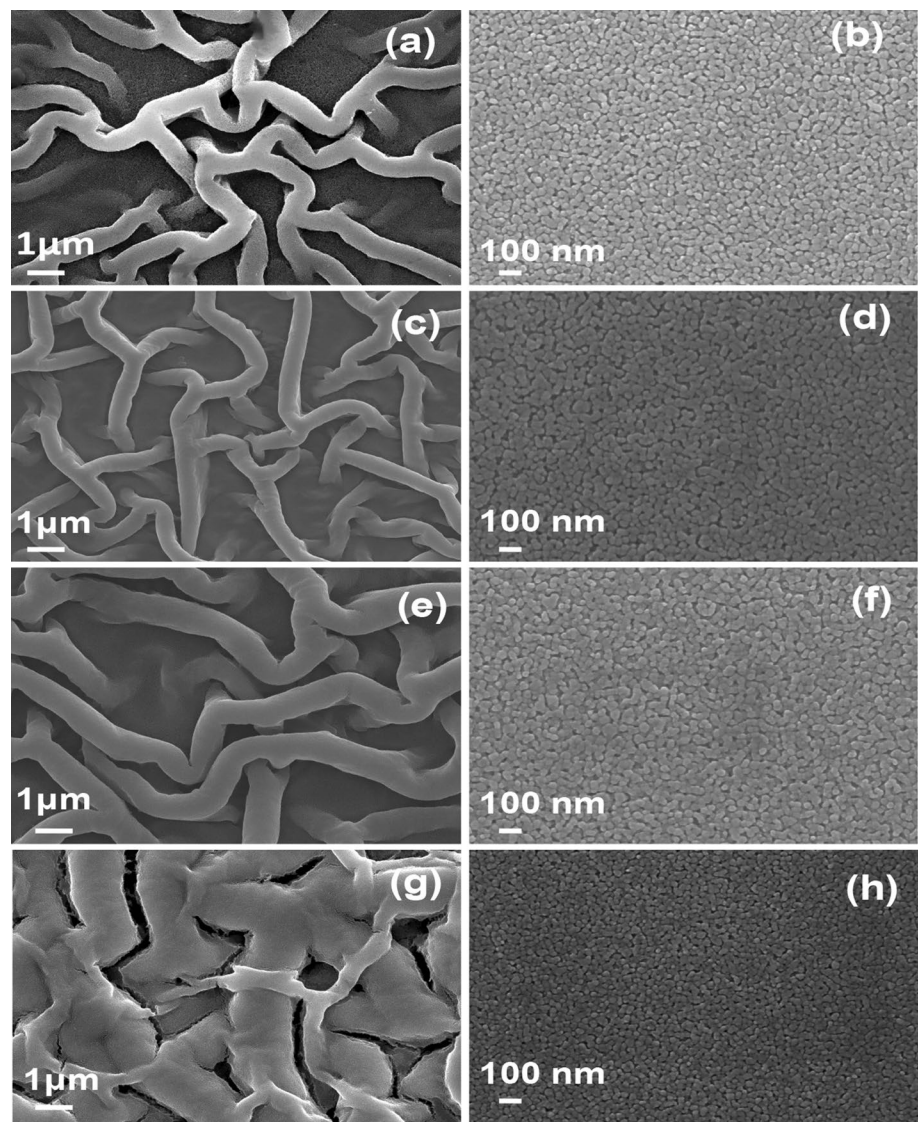


Fig. 4 Optical parameters of $\text{Cd}_y\text{Zn}_{1-y}\text{O}$ (CZ-1, CZ-2, CZ-3, CZ-4) thin films on the glass substrate with respect to air, **a** transmittance and **b** Tauc's plot for bandgap calculation

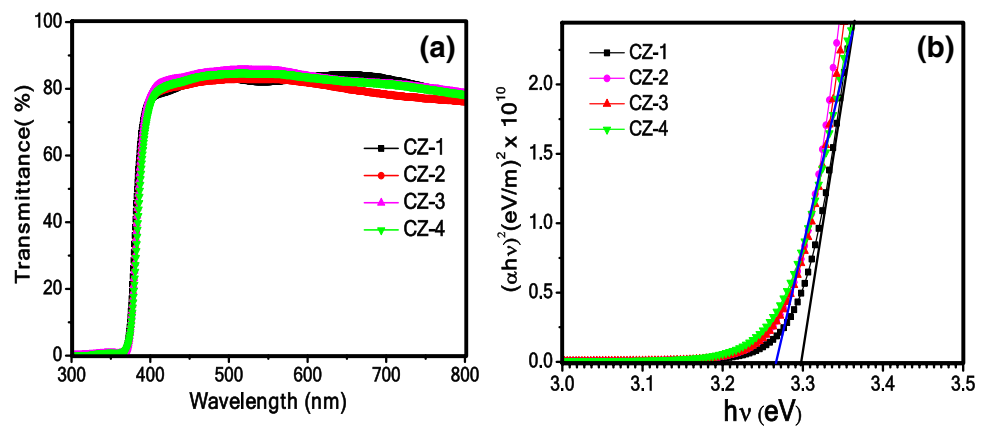
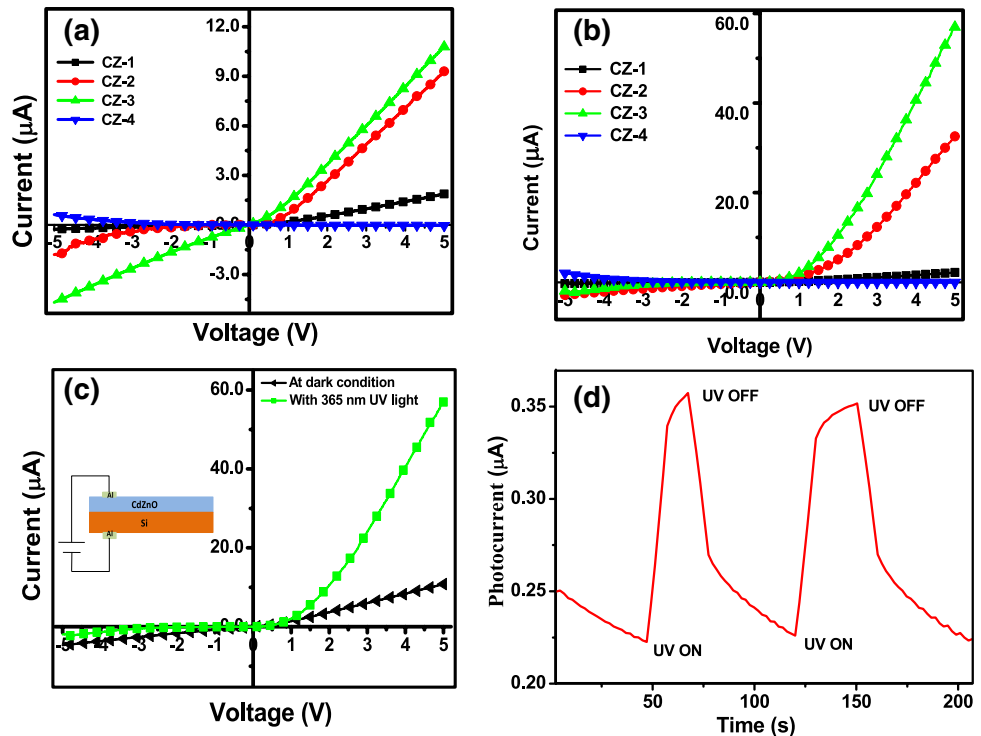


Fig. 5 I–V characteristics of the *n*-Cd_yZn_{1-y}O/*p*-Si heterojunction (CZ-1, CZ-2, CZ-3, CZ-4): **a** dark, **b** UV light (365 nm), **c** under dark and UV light (365 nm) *n*-Cd_yZn_{1-y}O/*p*-Si (*y* = 1 at%) heterojunction (CZ-3) and **(d)** growth and decay of the photoresponse of *n*-Cd_yZn_{1-y}O/*p*-Si (*y* = 1 at%) heterojunction (CZ-3)



with further increase in dopant content. The decrease in the resistivity may be due to the substitution of dopant ions at Zn²⁺ sites. With increasing the doping level, more dopant atoms occupy the zinc lattice sites, but after a certain level, the dopant atoms do not able to occupy more lattice sites and they have tendency to occupy interstitial sites where they form neutral defects and become ineffective as dopant impurities. So the electrical resistivity seems to be related to dopant concentration. The diode parameters such as reverse saturation current, ideality factor and barrier height were measured from I–V characteristic and are shown in Table 2 [39, 40]. In a similar study, Tataroglu et al. [22] have reported ideality factor and potential barrier values of Cd_{0.4}Zn_{0.60}O/*p*-Si heterojunction diode about 5.80 and 0.80 eV, respectively. Kumar et al. [28] have reported ideality factor and potential barrier values 1.63 and 0.40 eV, respectively, in case of n-type aluminium–boron-co-doped ZnO on *p*-type silicon (*n*-AZB/*p*-Si) heterojunction. The responsivity (*R*) was estimated from Eq. (1),

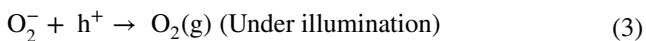
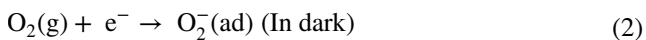
$$R = \frac{I_{ph}}{I_{inc}} \tag{1}$$

where *I*_{ph} is the photocurrent and *I*_{inc} is the incident UV light (365 nm) [41]. The device was illuminated with UV light (365 nm). The responsivity (*R*) of the prepared photodiode is shown in Table 2. The high responsivity was observed around 0.0126 A/W for CZ3 samples. The growth and decay of photoresponse for the photodiode have been obtained at bias of 4 V and are shown in Fig. 5d. The prepared photodiode exhibits highly repeatable photoresponse property, with a stable output. The illumination of UV light had been turned on and an exponential increase in response was obtained. The response was almost stable, with photocurrent saturation. This is due to the presence of surface states in the polycrystalline ZnO films, which is also supported by the diode characteristics. The rise time of the prepared photodiode was 11 s and decay time was 18 s as shown in Fig. 5d, which can be used in optical switching application.

Table 2 The electrical and photodetection properties of Cd_yZn_{1-y}O/*p*-Si heterojunctions

Sample code	Ideality factor (<i>η</i>)	Saturation current (A)	Barrier height (<i>Φ</i> _b) (eV)	Responsivity (<i>R</i>) (A/W)
CZ-1	2.90	3.30 × 10 ⁻¹⁰	0.76	0.0004
CZ-2	2.45	6.46 × 10 ⁻¹⁰	0.71	0.0072
CZ-3	2.53	1.89 × 10 ⁻⁸	0.70	0.0126
CZ-4	4.17	6.19 × 10 ⁻¹³	0.87	0.0002

The oxygen-assisted mechanism is main factor affecting the detection.



As the surface-to-volume ratio of nanostructured device is exceptionally high, they tend to absorb large number of oxygen atoms on surface defect states. The absorbed oxygen atoms become negatively charged by absorbing electrons from active material of the device, as shown in Eq. (2). In this way, photogenerated holes are captured in oxygen adsorbed on surface defect states, as shown in Eq. (3) and recombination of trapped holes and photogenerated electrons is delayed hence, response of the detector becomes slower [42]. The mechanism of UV light detection has been explained in our previous work [39]. This clearly shows that the cadmium as dopant material in ZnO can be an excellent material for optoelectronic devices [41, 43, 44].

4 Conclusion

$n\text{-Cd}_y\text{Zn}_{1-y}\text{O}/p\text{-Si}$ ($y=0, 0.5, 1, 1.5$ at%) heterojunctions were successfully fabricated using sol–gel spin coating method. All the thin films have wurtzite structure (002) without phase segregation after Cd doping. The wrinkle-type morphology composed with spherical grains was formed in heterojunctions. On increasing the concentration of Cd, the optical bandgap of ZnO thin films decreases. The highest electrical conductivity of heterojunction was observed in middle range (1 at%) of Cd atoms with good rectifying behaviour. Interestingly, the Cd contents on ZnO were found useful to enhance UV photodetection properties and the $\text{Cd}_y\text{Zn}_{1-y}\text{O}$ ($y=1$ at%) shows highest responsivity on exposure of UV light at bias 4 V. Moreover, the photodiode exhibits a sharp change in electrical conductivity after switching on UV source with fast response and recovery time. The results are encouraging because of good photoresponse behaviour of porous-shaped $n\text{-Cd}_y\text{Zn}_{1-y}\text{O}/p\text{-Si}$ heterojunctions and can be used as an optical sensor in optoelectronic applications.

Acknowledgements The first author (Vijay S Rana) is thankful to UGC, New Delhi, Govt. of India, for financial support (F.No. 16-9 (June 2017)/2018 (NET/CSIR);1480/CSIR-UGC NET JUNE 2017).

Declarations

Conflict of interest There is no conflict of interest. Entire research work has been done in the Semiconductor Research Lab, Department of Physics, Gurukula Kangri University, Haridwar, India.

References

- N.N. Jandow, Characteristics of ZnO MSM UV photodetector with Ni contact electrodes on polypropylene carbonate (PPC) plastic substrate. *Curr. Appl. Phys.* **10**, 1452–1455 (2010)
- S.J. Young, L.W. Ji, S.J. Chang, S.H. Liang, K.T. Lam, T.H. Fang, K.J. Chen, X.L. Du, Q.K. Xue, *Sensors Actuators A* **135**, 529–533 (2007)
- A. Raffiepour, F. Ghamari, A. Mohammadbeigi, M. Asghari, *Ann. Med. Health Sci. Res.* **2**, 129–133 (2015)
- E.M. Silvia, Q.W. Steven, *Rev. Environ. Health* **29**, 265–273 (2014)
- P.K. Maity, *Int. J. Dev. Res.* **6**, 8884–8889 (2016)
- P.H. Hart, S. Gorman, J.J.F. Jones, *Nat. Rev. Immunol.* **11**, 584–596 (2011)
- A.M. Selman, Z. Hassan, *Sensors Actuators A* **221**, 15–21 (2015)
- H.Y. Lee, C.T. Su, B.K. Wu, W.L. Xu, Y.J. Lin, M.Y. Chern, *J. Appl. Phys.* **109**, 113526 (2011)
- L. Liu, C. Yang, A. Patane, Z. Yu, F. Yang, L. Zhao, *R. Soc. Chem.* **9**, 8142–8148 (2017)
- S. Aksoy, Y. Caglar, *Superlattices Microstruct.* **51**, 613–625 (2012)
- N.H. Al-Hardan, M.A.A. Hamid, N.M. Ahmed, R. Shamsudin, N.K. Othman, *Sensors Actuators A* **242**, 50–57 (2016)
- K. You, *Appl. Phys. Lett.* **100**, 109–121 (2012)
- Y.S. Choi, J.W. Kang, D.K. Hwang, S.J. Park, *IEEE Trans. Electron Devices* **57**, 26–41 (2010)
- A.J. Gimenez, J.M.Y. Limón, J.M. Seminario, *J. Phys. Chem. C* **115**, 282–287 (2011)
- C.Y. Huang, Y.J. Yang, J.Y. Chen, C.H. Wang, Y.F. Chen, L.S. Hong, C.S. Liu, C.Y. Wu, *Appl. Phys. Lett.* **97**, 013503 (2010)
- H.Q. Le, S.J. Chua, *Journal of Physics D* **44**, 104–125 (2011)
- M. Dutta, T. Ghosh, D. Basak, *J. Electron. Mater.* **38**, 2335–2342 (2009)
- A. Singh, D. Kumar, P.K. Khanna, A. Kumar, M. Kumar, *J. Electrochem. Soc.* **158**, 9–12 (2011)
- V.S. Rana, J.K. Rajput, T.K. Pathak, L.P. Purohit, *J. Alloy. Compd.* **764**, 724–729 (2018)
- R.S. Ajimsha, M.K. Jayaraj, L.M. Kukreja, *J. Electron. Mater.* **37**, 770–775 (2008)
- J.K. Rajput, T.K. Pathak, V. Kumar, H.C. Swart, L.P. Purohit, *Phys. B* **535**, 314–318 (2018)
- A. Tataroglu, H. Aydın, A. Ahmed, A. Ghamdi, F.E. Tantawy, W.A. Farooq, F. Yakuphanoglu, *J. Electroceram.* **32**, 369–375 (2014)
- A. Singh, D. Kumar, P.K. Khanna, B.C. Joshi, M. Kumar, *Appl. Surf. Sci.* **258**, 1881–1887 (2011)
- A.A. Ziabari, F.E. Ghodsi, *Thin Solid Films* **520**, 1228–1232 (2011)
- J.K. Rajput, T.K. Pathak, V. Kumar, L.P. Purohit, *Appl. Surf. Sci.* **409**, 8–16 (2017)
- T.K. Pathak, J.K. Rajput, V. Kumar, L.P. Purohit, H.C. Swart, R.E. Kroon, *J. Colloid Interface Sci.* **487**, 378–387 (2017)
- B.D. Boruah, *Nanoscale Adv.* **1**, 2059–2085 (2019)
- V. Kumar, N. Singh, A. Kapoor, O.M. Ntwaeaborwa, *Mater. Res. Bull.* **48**, 4596–4600 (2013)
- N.H. Al-Hardana, A. Jalara, M.A.A. Hamid, L.K. Kengb, N.M. Ahmed, R. Shamsudin, *Sensors Actuators A* **207**, 61–66 (2014)
- A. Singh, J. Deshwal, D. Kumar, P.K. Khanna, M. Kumar, *ECS Trans.* **45**, 179–188 (2012)
- H. Huang, *Appl. Phys. Lett.* **94**, 063512 (2009)
- V.K. Sahu, *Phys. Express* **3**, 1–7 (2013)
- Y. Fahrettin, C. Yasemin, C. Mujdat, I. Saliha, *Mater. Sci. Semicond. Process.* **13**, 137–140 (2010)

34. F. Yakuphanoglu, S. Ilican, M. Caglar, Y. Caglar, *Superlattices Microstruct.* **47**, 732–743 (2010)
35. A.D. Acharya, S. Moghe, R. Panda, S.B. Shrivastava, M. Gangrade, T. Shripathi, D.M. Phase, V. Ganesan, *Thin Solid Films* **525**, 49–55 (2012)
36. T.H. Flemban, M.A. Haque, I. Ajia, N. Alwadai, S. Mitra, T. Wu, I.S. Roqan, *ACS Appl. Mater. Interfaces* **9**, 37120–37127 (2017)
37. L. Xu, G. Zheng, L. Zhao, S. Pei, *J. Lumin.* **158**, 396–400 (2015)
38. A. Bougrine, M. Addou, A. Kachouane, J.C. Bernede, M. Morsli, *Mater. Chem. Phys.* **91**, 247–252 (2005)
39. V.S. Rana, J.K. Rajput, T.K. Pathak, L.P. Purohit, *Colloids Surf. A* **586**, 124103 (2020)
40. V.S. Rana, J.K. Rajput, T.K. Pathak, L.P. Purohit, *Thin Solid Films* **679**, 79–85 (2019)
41. S. Sharma, C. Periasamy, *Superlattices Microstruct.* **73**, 12–21 (2014)
42. P. Pataniya, C.K. Zankat, M. Tannarana, C.K. Sumesh, S. Narayan, G.K. Solanki, K.D. Patel, V.M. Pathak, P.K. Jha, A.C.S. *Appl. Nano Mater.* **2**, 2758–2766 (2019)
43. R.E. Welsler, A.W. Sood, J. Cho, E.F. Schubert, J.L. Harvey, N.K. Dhar, A.K. Sood, *MRS Online Proc. Libr.* **1493**, 123–128 (2012)
44. A. Patsha, R. Pandian, S. Dhara, A.K. Tyagi, *J. Phys. D Appl. Phys.* **48**, 395102 (2015)

Publisher's Note Springer Nature remains neutral with regard to jurisdictional claims in published maps and institutional affiliations.